Applications of a new computational model of interface and phase-field fracture

Roman Vodička[1]

[1]*Faculty of Civil Engineering, Technical University of Košice*
Vysokoškolská 4, 04200 Košice, Slovakia
roman.vodicka@tuke.sk

Abstract. Computational analysis of fracture in multi-domain structures is considered so that cracks may appear in material bulks and also along material interfaces. The proposed computational model introduces two independent damage parameters relying on representation of rupture by mechanical damage theory. One of them being pertinent to the interface considering it as a negligibly thin adhesive layer of a contact zone between structural components. The arising interface cracks are supposed to appear so that cohesive zone models with general stress-strain relationships are implemented. The other damage parameter defined for the bulks uses the theory of phase-field fracture which causes elastic properties degradation only in a narrow material strip that forms a diffused crack. Both of these damaging schemes are expressed in terms of a quasi-static energy evolution process. Having such an energy formulation, the proposed computational approach is introduced in a variational form. The solution evolution being approximated by a semi-implicit time stepping procedure related to a separation of deformation and damage variables. The deformation and damage solutions at each instant being obtained by non-linear programming algorithms implemented together within a MATLAB finite element code. The numerical simulations with the model include an analysis of fibre separation arising in a fibre-reinforced composite material.

Keywords: Interface crack, Diffuse crack, Inclusion, Numerical simulation, Staggered scheme

1 Introduction

Many engineering material are composite, consisting of fibres or other inclusions and a matrix material which surrounds them. As in other types of materials, also in these an excess of loading forces may cause crucial changes in the material structure and may be followed by a loss of functionality. Anyhow, these changes may lead to a macroscopic evidences observed as cracks in material, debonding of structural components etc. Physical models which describe such cases introduce damage of materials leading subsequently to fracture. Efficient computational algorithms covering analysis of described kind of material deterioration are highly required.

The cracks may arise under various conditions, but they appear either inside material or along material interfaces. The computational methods should be able to capture both situations, which is also the case of the present approach.

The computational model is formulated in terms of material damage, where the degradation of the material properties explained as formation and cumulation of micro-cracks or micro-voids is described by internal variables, see e. g. works of Frémond [1], Maugin [2], which express the actual state of material properties or of adhesive joints between them. Anyhow, approaching the defined limit values of such internal variables means new crack arising or existing crack growth.

As other nonlinear phenomena, also damage and fracture can be formulated in terms of energies, allowing for a variational solution techniques. Recently, there were presented several such approaches for solving quasi-static problems, see e. g. author's works Vodička [3], Vodička and Mantič [4], Vodička [5], with interface cracks defined in a manner of cohesive zone models (CZM) described by Ortiz and Pandolfi [6], Park and Paulino [7] and their modifications. An advantage of the interface cracks is knowledge of their possible paths. Keeping the same variational philosophy introduced by Francfort et al. [8] also with material cracks, whose path need not be known, their propagation can be simulated by a damage phase-field model (PFM) as can be seen in works of Miehe et al.

[9], Paggi and Reinoso [10], Tanné et al. [11]. These cracks are also called diffuse as they relate distribution of a scalar material damage variable, represented by an at least continuous function, to presence of a crack in the material. This continuous smearing is a payment for not knowing in which direction the crack tends to propagate.

In the following sections, first, the model in terms of energies is described and governing relations for its energy state evolution are formulated. Then, selected aspects of the model discretisation and of its numerical analysis are stressed. Finally, the behaviour of the presented model and its computational implementation are documented in academic numerical tests which contain analysed domain with one or two inclusions.

2 The model of interface and phase-field fracture

Let us consider a bounded domain Ω which contains at least one inclusion as it is shown in Fig. 1 for a domain with one inclusion Ω^A and a matrix domain Ω^B. The respective boundaries are denoted Γ^A and Γ^B, the common part of the boundaries, an interface or a contact zone, is denoted Γ_i.

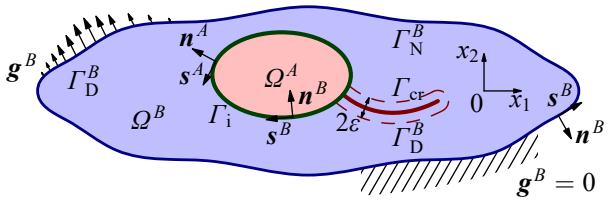

Figure 1. Description of the domain, cracks, boundary conditions and constraints.

Each of the boundaries Γ^A and Γ^B (besides Γ_i) is additionally disjointly split according to boundary conditions: Γ_D denotes the part with given displacements $\boldsymbol{u}$ introduced by a known function $\boldsymbol{g}$, and Γ_N with tractions $\boldsymbol{p}$ supposed to be prescribed. As far as only displacement loading is considered, tractions may be prescribed only by zeros on free parts of boundaries. The function $\boldsymbol{g}$ may be time dependent, the time variable is denoted by t.

The state of the structure, described by its energy state, evolves as long as the boundary conditions change in time. Let us consider a quasi-static evolution. The state is described by the displacement field $\boldsymbol{u}$ in the interior of the domains, the gap of displacements $[\![\boldsymbol{u}]\!]$ along interfaces, and two internal parameters α and ζ characterising current damage state which vary between 0 and 1, c. f. Francfort et al. [8], Miehe et al. [9]. Here, the parameter α determines the damage state derived from the damage PFM in the interior of the domains so that the value 0 corresponds to the undamaged state and the maximal value 1 belongs to the total damage, meant as a crack. Accordingly, the parameter ζ characterises the interface, considered as a negligibly thin adhesive layer, in the same manner with the value 0 corresponding to the undamaged adhesive and the value 1 pertaining to an interface crack (a crack along Γ_i).

The energy state is described by energy functionals. First, it includes the free energy represented by the (here plain strain) elastic stored energy $\mathfrak{E}$ of the domains and of the interfaces which may be taken into account as follows:

$$\mathfrak{E}\,(t;\boldsymbol{u},\alpha,\zeta) = \sum_{\eta=A,B}\int_{\Omega^\eta} \Phi(\alpha^\eta)\left(K\left|\mathrm{sph}^+\mathsf{e}(\boldsymbol{u}^\eta)\right|^2 + \mu\left|\mathrm{dev}\,\mathsf{e}(\boldsymbol{u}^\eta)\right|^2\right) + K\left|\mathrm{sph}^-\mathsf{e}(\boldsymbol{u}^\eta)\right|^2 + \frac{3}{8}G_\mathrm{c}\left(\frac{1}{\varepsilon}\alpha^\eta + \varepsilon\left(\nabla\alpha^\eta\right)^2\right)\mathrm{d}x + \int_{\Gamma_\mathrm{i}}\frac{1}{2}\left(\kappa\phi(\zeta)[\![\boldsymbol{u}]\!]\right)\cdot[\![\boldsymbol{u}]\!] + \frac{1}{2}\kappa_\mathrm{G}\left([\![\boldsymbol{u}]\!]_\mathsf{n}^-\right)^2 + G_\mathrm{c}^\mathrm{i}\zeta\,\mathrm{d}s, \quad (1)$$

valid for an admissible displacement field $\boldsymbol{u}$, i. e. such function that satisfies the displacement boundary conditions on Γ_D: $\boldsymbol{u} = \boldsymbol{g}(t)$, and for admissible damage parameters α and ζ, i. e. their values lying in the interval $[0,1]$. The non-admissible states have infinite energy $\mathfrak{E}$.

The parameters introduced in eq. (1) include stiffness characteristics of the domain materials which are represented in the current functional by the (plain strain) bulk modulus K and the shear modulus μ, then the initial stiffness κ of the undamaged adhesive layer and the compressive stiffness κ_G of this layer to replace the standard Signiorini contact condition by a normal stiffness penalisation term. The bulk elastic energy is decomposed using spherical part $\mathrm{sph}\,\mathsf{e}$ and deviatoric part $\mathrm{dev}\,\mathsf{e}$ of the small strain tensor e in order to see the possibility of different material degradation related to volumetric or shear strain. Simultaneously, tensile and compressive deformation

state may cause different material behaviour. If supposed that no damage propagation is allowed in purely compressive state, negative values of $\mathrm{sph}\,\mathsf{e}$, denoted here $\mathrm{sph}^{-}\mathsf{e}$ (similarly $\mathrm{sph}^{+}\mathsf{e}$ is introduced) do not imply degradation of the material.

The functions $\Phi(\alpha)$ and $\phi(\zeta)$ are degradation functions for elastic parameters of the domain (related to a PFM) and interface (related to a CZM), respectively. They determine how the stiffness of the material decreases during the damage process. Further, the energy accumulated due to a new crack requires fracture energy for domain cracks G_{c}, and fracture energy for the interface cracks $G_{\mathrm{c}}^{\mathrm{i}}$. Standardly in Griffith-like models, the term $\int_{\Gamma_{\mathrm{cr}}} G_{\mathrm{c}}\,\mathrm{d}s$ is used for expressing this energy over Γ_{cr} shown in Fig. 1. Here, it is replaced, as shown also by Tanné et al. [11], by a regularised functional (the term containing G_{c} in eq. (1)) controlling the evolution of the damage PFM diffuse crack, where ε is a characteristic length for PFM setting up the band of crack smearing as shown in Fig. 1.

Next, a part of energy due to the crack propagation is usually dissipated from the structure. Though, all energy related to creation of new cracks is involved into the stored energy in the present model, it is still necessary to guarantee a unidirectional character of the damage process (damage is accumulating thus damage parameters may only increase) at least by an assumption that there is no additional dissipated energy. This can be expressed as a potential $\mathfrak{R}(\dot\alpha,\dot\zeta)=0$ provided that $\dot\zeta\geq 0$ on Γ_{i}, and $\dot\alpha\geq 0$ in Ω. Impossibility of other states is enforced by infinite value of $\mathfrak{R}$.

The relations which govern the evolution can be written in a form of nonlinear variational inclusions

$$\begin{aligned}\partial_{\boldsymbol{u}}\mathfrak{E}(t;\boldsymbol{u},\alpha,\zeta)\ &\ni 0,\\ \partial_{\dot\alpha}\mathfrak{R}(\dot\alpha,\dot\zeta)+\partial_{\alpha}\mathfrak{E}(t;\boldsymbol{u},\alpha,\zeta)\ &\ni 0,\\ \partial_{\dot\zeta}\mathfrak{R}(\dot\alpha,\dot\zeta)+\partial_{\zeta}\mathfrak{E}(t;\boldsymbol{u},\alpha,\zeta)\ &\ni 0,\end{aligned}\tag{2}$$

where ∂ generally denotes a partial subdifferential as the functionals does not have to be smooth, e. g. $\mathfrak{R}$ jumps from zero to infinity. For smooth functionals, subdifferentials can be replaced by Gateaux differentials and the inclusions by equations. Along with the described relations, initial conditions for the state variables have to be taken into account:

$$\boldsymbol{u}^{\eta}(0,\cdot)=\boldsymbol{u}_0^{\eta},\quad \alpha^{\eta}(0,\cdot)=\alpha_0^{\eta}=0\quad \text{in } \Omega^{\eta},\qquad \zeta(0,\cdot)=\zeta_0=0\quad \text{on } \Gamma_{\mathrm{i}},\tag{3}$$

corresponding to an undamaged state.

2.1 Comments on numerical approaches

The problem is solved by the relations eq. (2) and eq. (3). It requires in its numerical solution both a time stepping algorithm and a spatial discretisation. The latter is implemented by a standard finite element approach using triangular or quadrilateral elements provided by Zienkiewicz et al. [12] and will not be discussed here. For the time discretisation, a variational character of the solved problem was intended to be kept. One of such possibilities includes a semi-implicit fractional-step method, referred in applications also as a staggered scheme, which relies on separate convexity of the energy functional eq. (1) with respect to deformation variables and damage variables. It means that the function $\mathfrak{E}(t;\boldsymbol{u},\alpha,\zeta)$ as a function of $\boldsymbol{u}$ is convex for all (α,ζ) fixed, and also as a function of the couple (α,ζ) it is convex for all $\boldsymbol{u}$ fixed.

For the time stepping, a fixed time step τ is chosen in a fixed time range $[0,T]$. The solution is obtained at the instants $t^k=k\tau$ for $k\in\{0,1,2,\dots,\lfloor T/\tau\rfloor\}$ and denoted $\boldsymbol{u}_\tau^k$ for displacements and α_τ^k, ζ_τ^k for the damage variables. Here, index 0 refers to the discretised initial conditions eq. (3). In the numerical version of eq. (2), the derivatives in the rate variables are approximated by the finite differences e. g. $\dot\zeta\approx\frac{\zeta_\tau^k-\zeta_\tau^{k-1}}{\tau}$, and the differentiation with respect to pertinent rate is accordingly replaced by the differentiation with respect to the value of the state variable at the step k, e. g. ζ_τ^k. These approximations then provide the system from eq. (2) in the following form:

$$\begin{aligned}\partial_{\boldsymbol{u}_\tau}\mathfrak{E}(k\tau;\boldsymbol{u}_\tau,\alpha_\tau^{k-1},\zeta_\tau^{k-1})\ &\ni 0,\\ \tau\,\partial_{\alpha_\tau}\mathfrak{R}\Big(\frac{\alpha_\tau-\alpha_\tau^{k-1}}{\tau},\frac{\zeta_\tau-\zeta_\tau^{k-1}}{\tau}\Big)+\partial_{\alpha_\tau}\mathfrak{E}\big(k\tau;\boldsymbol{u}_\tau^k,\alpha_\tau,\zeta_\tau\big)\ &\ni 0,\\ \tau\,\partial_{\zeta_\tau}\mathfrak{R}\Big(\frac{\alpha_\tau-\alpha_\tau^{k-1}}{\tau},\frac{\zeta_\tau-\zeta_\tau^{k-1}}{\tau}\Big)+\partial_{\zeta_\tau}\mathfrak{E}\big(k\tau;\boldsymbol{u}_\tau^k,\alpha_\tau,\zeta_\tau\big)\ &\ni 0.\end{aligned}\tag{4}$$

The separation of variables in the staggered algorithm provides two minimisations to be performed at each time step. Considering the simplified form of the dissipation functional $\mathfrak{R}$, the first minimisation with respect to the displacements of the functional

$$\mathfrak{H}_1^k(\boldsymbol{u}_\tau) = \mathfrak{E}(k\tau; \boldsymbol{u}_\tau, \alpha_\tau^{k-1}, \zeta_\tau^{k-1}) \tag{5}$$

provides $\boldsymbol{u}_\tau^k$ as its minimiser, i. e. $\boldsymbol{u}_\tau^k = \operatorname{argmin} \mathfrak{H}_1^k(\boldsymbol{u}_\tau)$, due to the first inclusion in eq. (4). It should be noted that the constraints for $\boldsymbol{u}_\tau$ (admissibility) are hidden in the definition of $\mathfrak{E}$.

The second minimisation includes constraints $\alpha_\tau^{k-1} \leq \alpha_\tau \leq 1$ and $\zeta_\tau^{k-1} \leq \zeta_\tau \leq 1$, where the upper bounds come from the definition of $\mathfrak{E}$ (admissibility), and the lower bounds come from the definition of $\mathfrak{R}$. The pertinent functional

$$\mathfrak{H}_2^k(\alpha_\tau, \zeta_\tau) = \mathfrak{E}\big(k\tau; \boldsymbol{u}_\tau^k, \alpha_\tau, \zeta_\tau\big) \tag{6}$$

renders the minimiser $(\alpha_\tau^k, \zeta_\tau^k)$, i. e. $(\alpha_\tau^k, \zeta_\tau^k) = \operatorname{argmin} \mathfrak{H}_2^k(\alpha_\tau, \zeta_\tau)$, due to the second and third relations in eq. (4). These two minimisations of the decoupled system are solved recursively for all k, $k \in \{1, 2, \ldots, \lfloor T/\tau \rfloor\}$.

In the numerical implementation, the functional in eq. (5) is piecewise quadratic so that sequential quadratic programming algorithms can be used in its solution, see e. g. Nocedal and Wright [13], Dostál [14], Vodička et al. [15]. The functional in eq. (6) is convex, even could be quadratic, depending on the form of the degradation functions Φ and ϕ used in eq. (1). Anyhow, the sequential quadratic programming algorithms can be used even in this case.

3 Calculations

Interaction between interface and domain cracks is studied for two cases containing one or two inclusions. The schemes for these problems are shown in Fig. 2, where the plane strain deformation state is taken into account. It is considered either one centrally placed circular inclusion or two slightly unsymmetrically placed inclusions

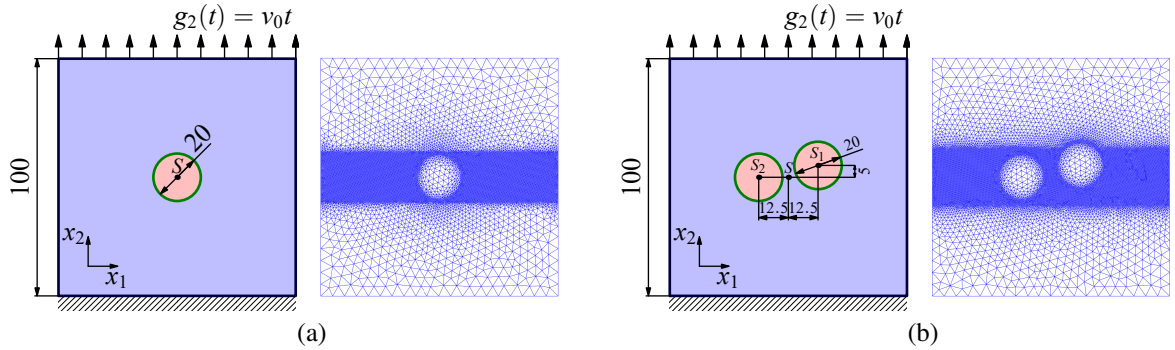

Figure 2. Schemes and meshes for the calculations with (a) one inclusion and (b) two inclusions.

within the same square domain. The initial elastic properties (introduced in eq. (1) for an undamaged material) are: $K^A = 52\,\text{GPa}$, $\mu^A = 29\,\text{GPa}$ (inclusions), $K^B = 3\,\text{GPa}$, $\mu^B = 1\,\text{GPa}$ (matrix), and $\kappa = \left(\begin{smallmatrix} 1 & 0 \\ 0 & 0.5 \end{smallmatrix}\right)\text{PPa}\,\text{m}^{-1}$, $\kappa_\text{G} = 1\,\text{EPa}\,\text{m}^{-1}$ at the interfaces. The mesh size (min.) in Fig. 2 is $h = 0.5\,\text{mm}$.

The fracture energy in all domains is $G_\text{c} = 1\,\text{kJm}^{-2}$, while that of the interfaces is $G_\text{c}^\text{i} = 1\,\text{Jm}^{-2}$. The vertical displacement loading $g_2(t) = v_0 t$ is increasing by the velocity $v_0 = 1\,\text{mms}^{-1}$, where the time step is 2 ms.

The degradation function Φ of PFM is chosen in a simple quadratic form: $\Phi(\alpha) = \big(\varepsilon_0^2 + (1-\alpha)^2\big)$, where the parameter ε_0 adjusts residual stiffness after total damage to avoid degeneration of the totally damaged material in the numerical solution. The interface degradation function ϕ of CZM is chosen to obey a bilinear model presented by Vodička and Mantič [4], which is given by the function $\phi(\zeta) = \frac{\beta(1-\zeta)}{\zeta+\beta}$ and the parameter $\beta = 0.1$ adjusts damage initiation and evolution processes.

In what follows some features of the fracture process are presented. First, there appears an interface opening crack which stops propagating when the interface normal traction is not able to reach the critical value. The

damage propagation in the sense of CZM appears in the region, where the value of the interface damage parameter ζ lies between its extreme values. In the same region, a stress distribution related to CZM can be observed. The used model guarantees according to Vodička and Mantič [4] maximum of the normal cohesive stress for the value $\sqrt{\frac{2\kappa_{\rm n}G_{\rm c}^{\rm i}\beta}{1+\beta}} = 13.8\,\text{MPa}$. Similarly, to initiate an opening crack of PFM it is necessary for the critical stress trace $\sigma_{\rm tr}$ to reach the level $\sqrt{\frac{3KG_{\rm c}}{2\varepsilon}} = 39.4\,\text{MPa}$, with ε chosen as 1 mm related to the characteristic material length as discussed by Tanné et al. [11]. All these explanations can be read also from the pictures in Fig. 3. Three instants

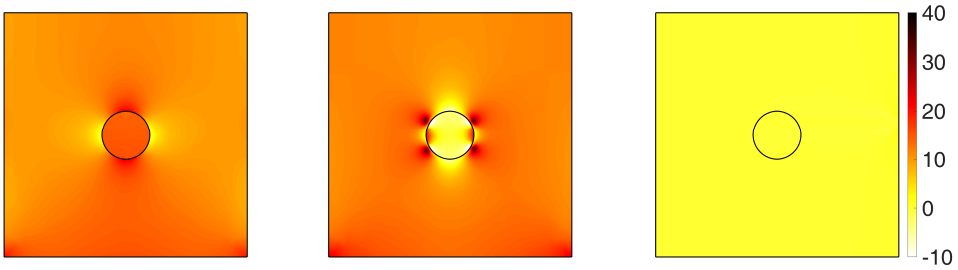

Figure 3. The stress trace $\sigma_{\rm tr}$ [MPa] distribution in the structure while the interface crack is propagating shown at the instants $t = 0.312\text{s}, 0.366\text{s}, 0.516\text{s}$.

are chosen: the first corresponds to the first separation of materials at the interface, the second documents stress concentration and initiation of phase-field fracture, the third contains the situation where the crack reached the outer contour.

The crack in the domain appears when the stress reaches the aforementioned value and it is propagating in the horizontal direction until it reaches the outer contour as it can be seen in Fig. 4 expressed in terms of the phase-field damage parameter α. The deformed shape of the structure also documents propagation of the interface

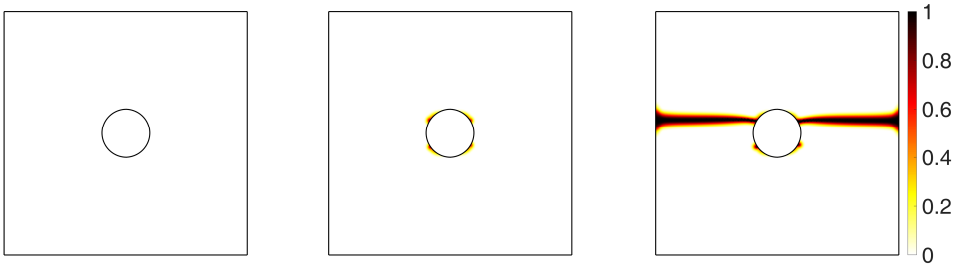

Figure 4. Phase-field damage α distribution in the structure while the interface crack is propagating shown at the same instants t as in Fig. 3.

crack. It is shown in Fig. 5 with magnified displacements. It presents also the values of equivalent shear strain $\epsilon_{\rm eq}$. In the PFM, there in fact remains totally destroyed material with negligible stiffness (determined by $\varepsilon_0 = 10^{-6}$ introduced in the degradation function Φ above), therefore the crack appears with large strain, though no stress.

Similar pictures are show for the second example with two inclusions. The stress traces are shown in Fig. 6, phase-field damage α is presented in Fig. 7, and equivalent shear strain $\epsilon_{\rm eq}$ drawn on magnified displacements is displayed Fig. 8. All these figures use the same selected instant plots: the first instant corresponds to the first interface crack formation, the second documents stress concentration and initiation of phase-field fracture, the third presents the crack between the inclusions, the fourth contains the situation where the crack reached the outer contour.

In both studied cases the parameters that affect the damage and crack propagation were set so that first there appeared an interface crack which subsequently invoked a crack in the material of matrix. Appropriate adjusting of these parameters, however, can lead to different scenarios which might appear in a wide range of technical problems.

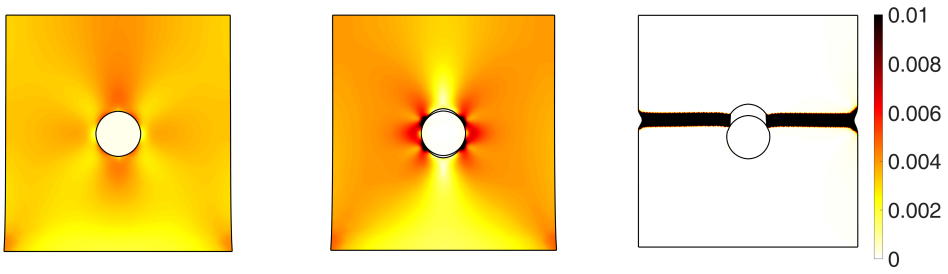

Figure 5. Shear strain magnitude $\epsilon_{\rm eq}$ distribution in the structure while the interface crack is propagating shown at the same instants t as in Fig. 3. Displacements are magnified 10 times.

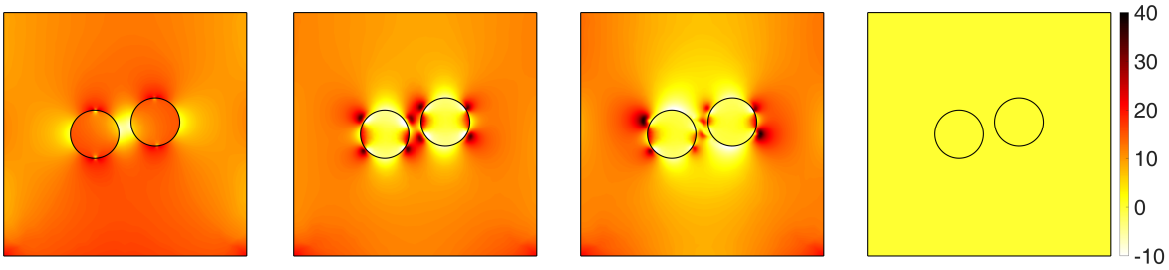

Figure 6. The stress trace $\sigma_{\rm tr}$ [MPa] distribution in the structure while the interface crack is propagating shown at the instants $t = 0.318$s, 0.360s, 0.370s, 0.462s.

4 Conclusions

A model for computations with cracks along interfaces and in domains has been described and tested. It allows a staggered modelling scheme with deformation and damage variables separated, guaranteeing thus a variational structure for the numerical approximation of the physical model. Naturally, the model includes a couple of parameters which should be appropriately adjusted in order to obtain results which comply with the experimental measurements. Nevertheless, based on the result of the current study, it is supposed that the approach may be successfully utilised also in more complex engineering calculations.

Acknowledgements. Author acknowledges support from The Ministry of Education, Science, Research and Sport of the Slovak Republic by the grants VEGA 1/0374/19 and VEGA 1/0363/21.

Authorship statement. The author hereby confirms that he is the sole liable person responsible for the authorship of this work, and that all material that has been herein included as part of the present paper is the property (and authorship) of the author.

References

[1] M. Frémond. Dissipation dans l'adhérence des solides. *C.R. Acad. Sci., Paris, Sér.II*, vol. 300, pp. 709–714, 1985.
[2] G. Maugin. The saga of internal variables of state in continuum thermo-mechanics (1893-2013). *Mech. Res. Commun.*, vol. 69, pp. 79–86, 2015.
[3] R. Vodička. A quasi-static interface damage model with cohesive cracks: SQP-SGBEM implementation. *Eng. Anal. Bound. Elem.*, vol. 62, pp. 123–140, 2016.
[4] R. Vodička and V. Mantič. An energy based formulation of a quasi-static interface damage model with a multilinear cohesive law. *Discrete Cont. Dyn. - S*, vol. 10, n. 6, pp. 1539–1561, 2017.
[5] R. Vodička. A new quasi-static delamination model with rate-dependence in interface damage and its operation under cyclic loading. *Int. J. Solids Struct.ures*, vol. 224, pp. 111035, 2021.
[6] M. Ortiz and A. Pandolfi. Finite-deformation irreversible cohesive elements for three-dimensional crack-propagation analysis. *Int. J. Numer. Meth. Eng.*, vol. 44, n. 9, pp. 1267–1282, 1999.

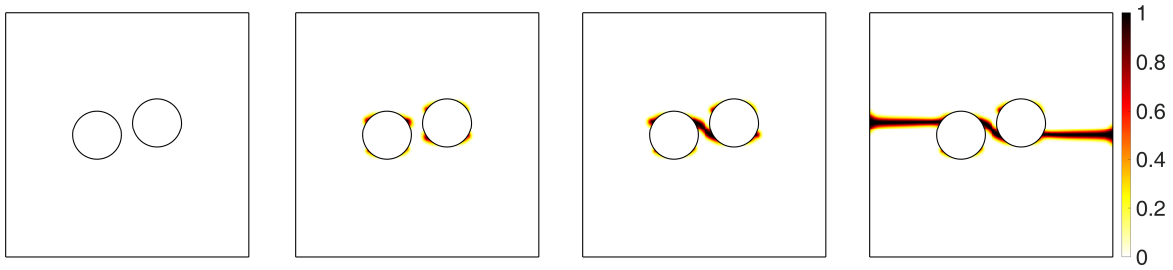

Figure 7. Phase-field damage α distribution in the structure while the interface crack is propagating shown at the same instants t as in Fig. 6.

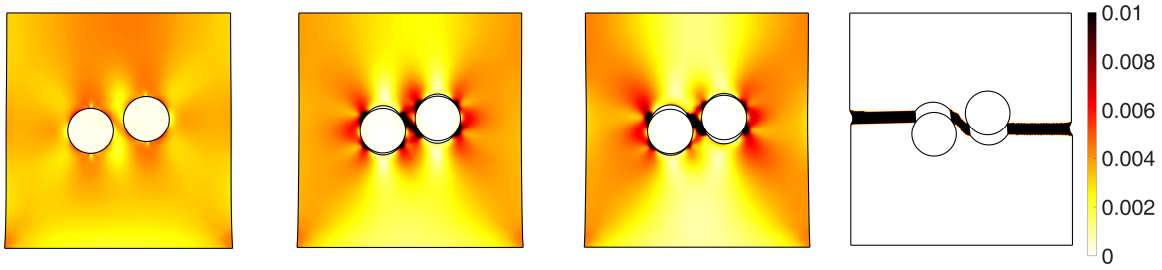

Figure 8. Shear strain magnitude ϵ_{eq} distribution in the structure while the interface crack is propagating shown at the same instants t as in Fig. 6. Displacements are magnified 10 times.

[7] K. Park and G. Paulino. Cohesive zone models: A critical review of traction-separation relationships across fracture surfaces. *Appl. Mech. Rev.*, vol. 64, n. 6, 2011.
[8] G. Francfort, B. Bourdin, and J.-J. Marigo. The variational approach to fracture. *J. Elasticity*, vol. 91, n. 1-3, pp. 5–148, 2008.
[9] C. Miehe, M. Hofacker, and F. Welschinger. A phase field model for rate-independent crack propagation: Robust algorithmic implementation based on operator splits. *Comput. Method. Appl. M.*, vol. 199, n. 45-48, pp. 2765–2778, 2010.
[10] M. Paggi and J. Reinoso. Revisiting the problem of a crack impinging on an interface: A modeling framework for the interaction between the phase field approach for brittle fracture and the interface cohesive zone model. *Comput. Method. Appl. M.*, vol. 321, pp. 145–172, 2017.
[11] E. Tanné, T. Li, B. Bourdin, J.-J. Marigo, and C. Maurini. Crack nucleation in variational phase-field models of brittle fracture. *J. Mech. Phys. Solids*, vol. 110, pp. 80–99, 2018.
[12] O. Zienkiewicz, R. Taylor, and J. Zhu. *The Finite Element Method: Its Basis and Fundamentals*. Butterworth-Heinemann, Oxford, UK, 7 edition, 2013.
[13] J. Nocedal and S. Wright. *Numerical Optimization*. Springer, New York, 2006.
[14] Z. Dostál. *Optimal Quadratic Programming Algorithms*, volume 23 of *Springer Optimization and Its Applications*. Springer, Berlin, 2009.
[15] R. Vodička, V. Mantič, and T. Roubíček. Energetic versus maximally-dissipative local solutions of a quasi-static rate-independent mixed-mode delamination model. *Meccanica*, vol. 49, n. 12, pp. 2933–2963, 2014.